A comparison between a child-size PMHS and the Hybrid III 6 YO in a sled frontal impact

Francisco J. Lopez-Valdes, Jason Forman, Richard Kent
University of Virginia, Center for Applied Biomechanics

Ola Bostrom
Autoliv Research

Maria Segui-Gomez
European Center for Injury Prevention, Universidad de Navarra

ABSTRACT – As pediatric PMHS data are extremely limited, evidence of kinematic differences between pediatric ATDs and live humans comes from comparison of laboratory data to field crash data. Despite the existence of regulations intended to prevent head injuries, these remain the most common serious injuries sustained by children in crashes. In this study, nine frontal sled tests using a Hybrid III 6YO and three tests performed with a child-size adult PMHS were compared, with focus on the kinematic responses (especially of the head) and the seatbelt forces generated during the impact. Two different restraint systems (a pretensioning, force-limiting seatbelt, and a non pretensioning force-limiting standard belt) and two different impact speeds (29 km/h and 48 km/h) were compared. Data from the PMHS were scaled using the erect sitting height of a 50th percentile 6YO and both scaled and unscaled data are presented. The ATD predicted correctly the peak values of the scaled displacements of the PMHS, but differences in relevant parameters such as torso angle and resultant acceleration at different locations were found between the dummy and the PMHS. The ATD's stiffer thoracic spine is hypothesized as a major cause of these differences.

INTRODUCTION

Head injuries are the most common serious injuries sustained by children in motor vehicle crashes, regardless of age, crash direction or restraint type [Arbogast et al, 2004; Arbogast et al, 2002; Sherwood et al, 2003]. Federal regulation FMVSS No. 213 in the United States and regulation ECE No. 44 in Europe limit the forward excursion and acceleration of the dummy's head permitted by child restraint systems sold in those regions. Despite these regulations, one third of all pediatric injuries are to the head [Adekoya et al., 2002; Thompson and Irby, 2003]. Reported mechanisms associated with these injuries include direct contact of the head with any of the interior structures of the car as well as non-contact inertial loading of the brain [Arbogast et al., 2002]. In either situation, the kinematics of the child's head during the crash are fundamentally related to the injury mechanism, and a precise understanding and ability to model the head motion is a critical requirement for effective design of countermeasures.

Pediatric injury tolerance data are scarce. To the knowledge of the authors, sled tests with pediatric post-mortem human subjects (pPMHS) have been performed only on 15 occasions using 11 pPMHS [Kallieris et al. 1976 and 1978, Wismans et al. 1979, Dejammes et al. 1984, Brun-Cassan et al. 1993, Mattern et al. 2002], and only six tests [Kallieris et al. 1976] involved booster seated pPMHS (the currently recommended restraint condition for the 6-year-old child) and the instrumentation and documentation of those tests does not reflect the state of the art *circa* 2009. Thus, while adult Anthropomorphic Test Devices (ATD) and their corresponding injury criteria are based on numerous tests with adult PMHS, the development of pediatric ATDs has relied primarily on scaled adult data.

This paper presents a comparison between a small size adult PMHS (with an anthropometry similar to a 10 year old child) with the Hybrid III 6 YO using state of the art instrumentation and visual documentation. A series of frontal sled tests was performed on both the PMHS and the ATD using different impact speeds (29 km/h and 48 km/h) and restraint systems (standard belt and booster seat; pre-tensioning, force-limiting belt and booster seat). The anthropometry of this subject presents a unique opportunity to generate basic biomechanical data to

aid in the assessment and design of more biofidelic pediatric ATDs.

The goal of this study is to compare the kinematic responses of the PMHS and the pediatric ATD in matched impact conditions over a range of speeds and restraint parameters.

METHODS

This study considers a total of 12 frontal sled tests. The Hybrid III 6YO ATD was used in nine of these tests, and the small PMHS in three.

Experimental setup

The occupant (Note: "occupant" will be used generically in this study to refer to either the PMHS or the ATD) was positioned in a booster seat (Model Step 3 Turbobooster, Graco) in the right rear seat position of a vehicle buck created from a 2004 model year mid-sized U.S. sedan. While the ATD was seated on a high back booster seat, a low back booster seat was used with the PMHS due to the larger anthropometry (primarily seated height) of the PMHS. The acceleration pulses were approximately trapezoidal (**Figure 1**) and represented the deceleration of the actual vehicle in a full frontal barrier test [Forman et al., 2006].

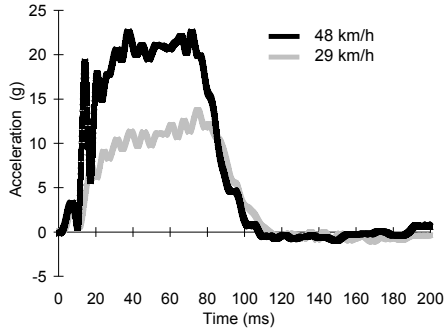

Figure 1 – Representative sled deceleration pulses.

The occupant was restrained using two different systems: a progressive, force-limiting (nominal 3 kN and 5 kN limits), pre-tensioning seatbelt (FL+PT) and a standard (not force-limiting or pretensioning) belt (SB). Tension on the seatbelt was measured (Eaton Leboy, Model Number 3419-3.5K) at the upper (between shoulder and retractor) and lower (above the buckle) shoulder belt and at the outboard lap belt. See Forman et al. (2008) for additional details. The seatbelt retractor mechanism was mounted on the rear deck of the vehicle (i.e., no D-ring was used). The rear seat cushion and the belt system were replaced after each test. The test matrix is shown in Table 1. All sensor data were sampled at 10 kHz and filtered according to SAE J211 recommendations.

Table 1 – Test matrix

Test number	Occupant type	Restraint	Impact speed (km/h)
1225, 1226, 1227	H3 6YO	SB	48
1303, 1304, 1306	H3 6YO	FL+PT	48
1307, 1308, 1309	H3 6YO	FL+PT	29
1384	PMHS #437	FL+PT	29
1385	PMHS #437	FL+PT	48
1388	PMHS #437	SB	48

Each test was recorded with two lateral off-board digital high speed cameras at 1000 frames per second. Trajectories of the occupants were determined in the buck reference frame (XZ, see Figure 2) from the passenger-side (right-side) videos. Photo targets were placed on corresponding points in the ATD and the PMHS (head, shoulder, elbow, hip, knee, ankle). The trajectories of the photo targets were digitized manually using commercial analysis software (Phanton Camera Control, version 8.1.607, Vision Research, Inc.).

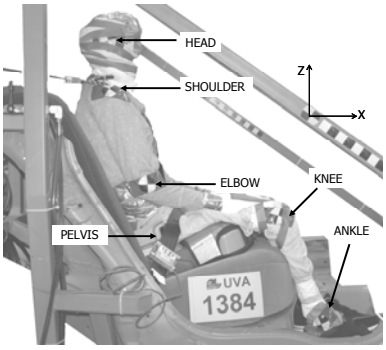

Figure 2 – PMHS positioned in buck and buck reference frame.

PMHS tests

The preparation, handling, and test procedure of the PMHS for the tests were performed according to the Protocol for the Handling of Biological Material of the Center for Applied Biomechanics and were approved by the University of Virginia Center for Applied Biomechanics Oversight Committee. Repeated tests were performed on the PMHS to maximize the information obtained from this rare subject. The test matrix was designed to minimize the effects of repeated tests by performing them in an order anticipated to minimize injury risk until the final test. Thus, no test at 29 km/h with the SB belt

was performed and the FL+PT condition was tested before the SB condition.

PMHS preparation and instrumentation. The subject presented a degenerative fracture of the T7 vertebral body prior to testing but no other significant bone pathology. Both cardiovascular and pulmonary systems were pressurized to a nominal *in vivo* value (approximated 10 kPa measured externally) during the tests. The center of gravity of the head was located using the method proposed by Robbins (1983). The PMHS was instrumented to measure triaxial acceleration (Endevco model 7264B) and triaxial angular velocity (DTS model ARS-12k) at the head and the first thoracic vertebra (T1). Triaxial acceleration was measured at the the thoracic spine (T9), lumbar spine (L2), and pelvis. A uniaxial accelerometer was installed on the sternum. Accelerometers were rigidly attached to bony structures by specifically designed mounts. Head acceleration, which was measured as part of a 6-degree-of-freedom cube (triaxial linear acceleration and triaxial angular rate) mounted at an arbitrary location on the head, was transformed using rigid body dynamics [Martin et al. 1998] to the center of gravity for reporting. Its components were projected in the orthogonal anatomical planes (sagittal, coronal, frontal). After Test 1388 a complete necropsy was performed on the PMHS.

ATD tests

The Hybrid III 6 YO was instrumented to measure triaxial acceleration at the head center of gravity (cg), chest cg, and pelvis. A detailed description of these tests can be found in Forman et al. (2008).

Scaling

The anthropometry of the PMHS was closer to a 10-year-old child than to a 6-year-old. Since the dummy used in the regulation FMVSS No. 213 is the HIII 6YO, data from the PMHS were scaled to represent the response of a 6 YO according to the procedure described by Eppinger et al. (1984). Since the body kinematics depends intrinsically on the length of the limbs, a length-based scaling method was used here. Table 2 compares the anthropometric characteristics of the subjects. As the main focus of the study was to analyze head and spine trajectories, the erect sitting height was chosen as the characteristic length for scaling. Thus, the scaling factors used in this study were:

$$\lambda_L = \frac{\hat{L}_{6YO}}{\hat{L}_{PMHS}} = 0.785 \qquad (1)$$

$$\lambda_t = \lambda_L \quad \lambda_a = \lambda_L^{-1} \quad \lambda_f = \lambda_L^2 \qquad (2)$$

$$magnitude_{scaled} = \lambda_{magnitude} magnitude_{PMHS} \qquad (3)$$

where L is length, t is time, a is acceleration, f is force and "magnitude" represents any of the previous. Equation (3) shows the relationship that governs the scaling from the PMHS to a 6YO child.

Table 2 - Anthropometry of the ATD, a 6YO 50th percentile and the PMHS (cm, kg).

	HIII 6 YO	6 YO 50^{th*}	PMHS	λ_L
Sitting Height Erect	63.5	64.4	82.0	0.785
Stature	114.0	118.1	147.0	0.803
Weight	23.41	21.45	27.2	na

* Source: Malina et al. (1965).

RESULTS

The injuries observed in the necropsy are summarized in Table 3.

Table 3 – Summary of injuries.

Injuries	AIS 2005
C7-T1: Partial tear of supraspinous ligament	640284.1
C7-T1: Interspinous ligament partially disrupted	640284.1
C7-T1: Near complete tear of ligamentum flavum	640284.1
C7 right transverse process fracture	650220.2
T1 right transverse process fracture	650420.2
T9 spinous process fracture	650418.2
T12 transverse process fracture	650420.2
L1 transverse process fracture	650420.2
Greater than 3 fractured ribs on boths sides without fail	450203.3
Right clavicle fracture	750751.2

Figure 3 shows the trajectories of the photo targets during the impact. The first column in Figure 3 shows the non-scaled trajectories of the photo targets while the scaled values are presented in the second column. At each speed and for each type of restraint, the comparison between the observed PMHS trajectories and the mean (± one standard deviation) of the dummy trajectories is presented. Though the external shape of the PMHS and the dummy are not the same, in order to ease the visualization and comparison of the data, the trajectories of the photo targets from the dummy have been imposed on the PMHS contour.

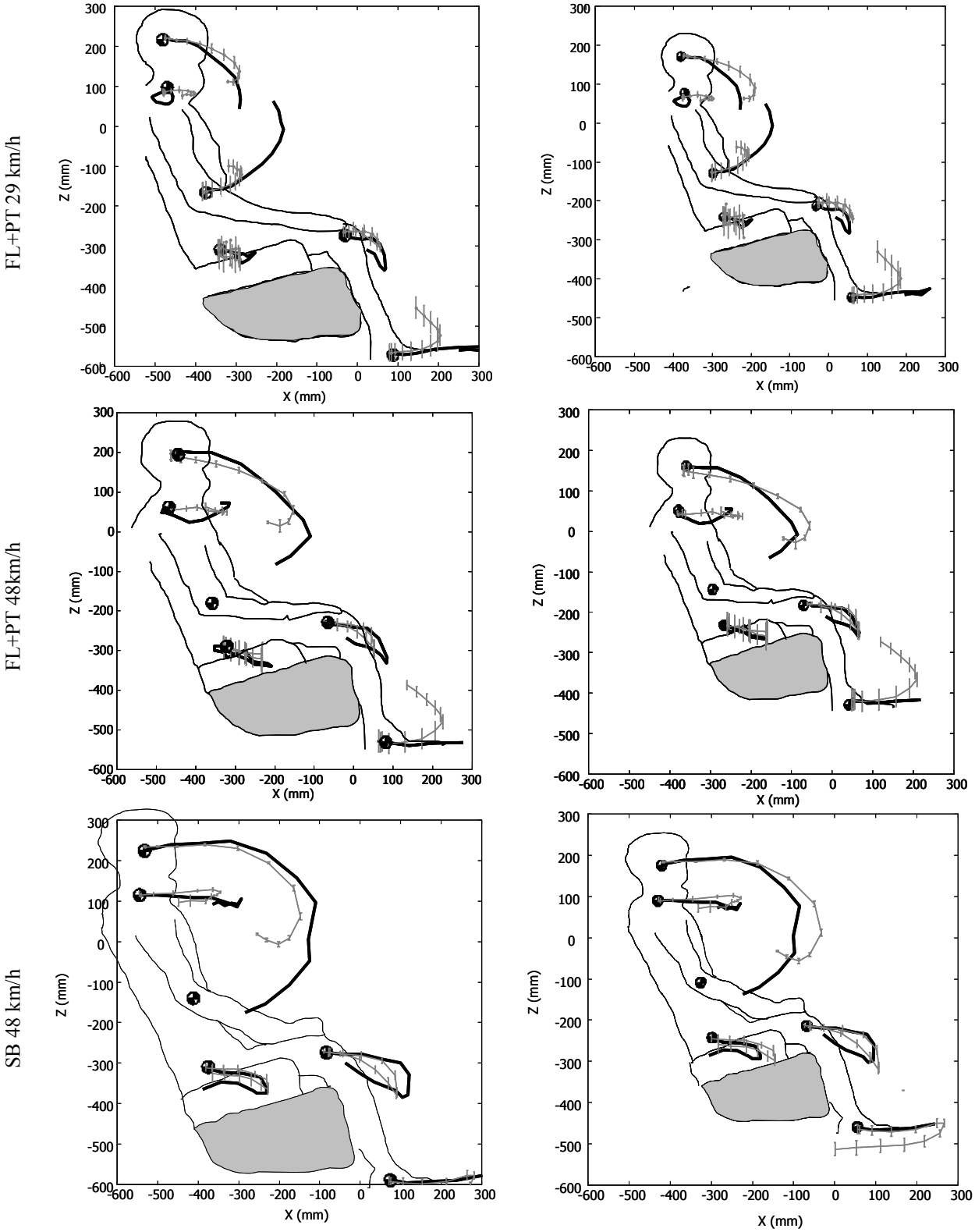

Figure 3 – Comparison of the trajectories of the photo targets on the ATD (grey: mean value and standard deviation) and on the PMHS (black). Un-scaled (left) and scaled (right) trajectories are presented for the PMHS. The origin of each ATD trajectory has been shifted to the origin of the corresponding PMHS trajectory to ease the comparison.

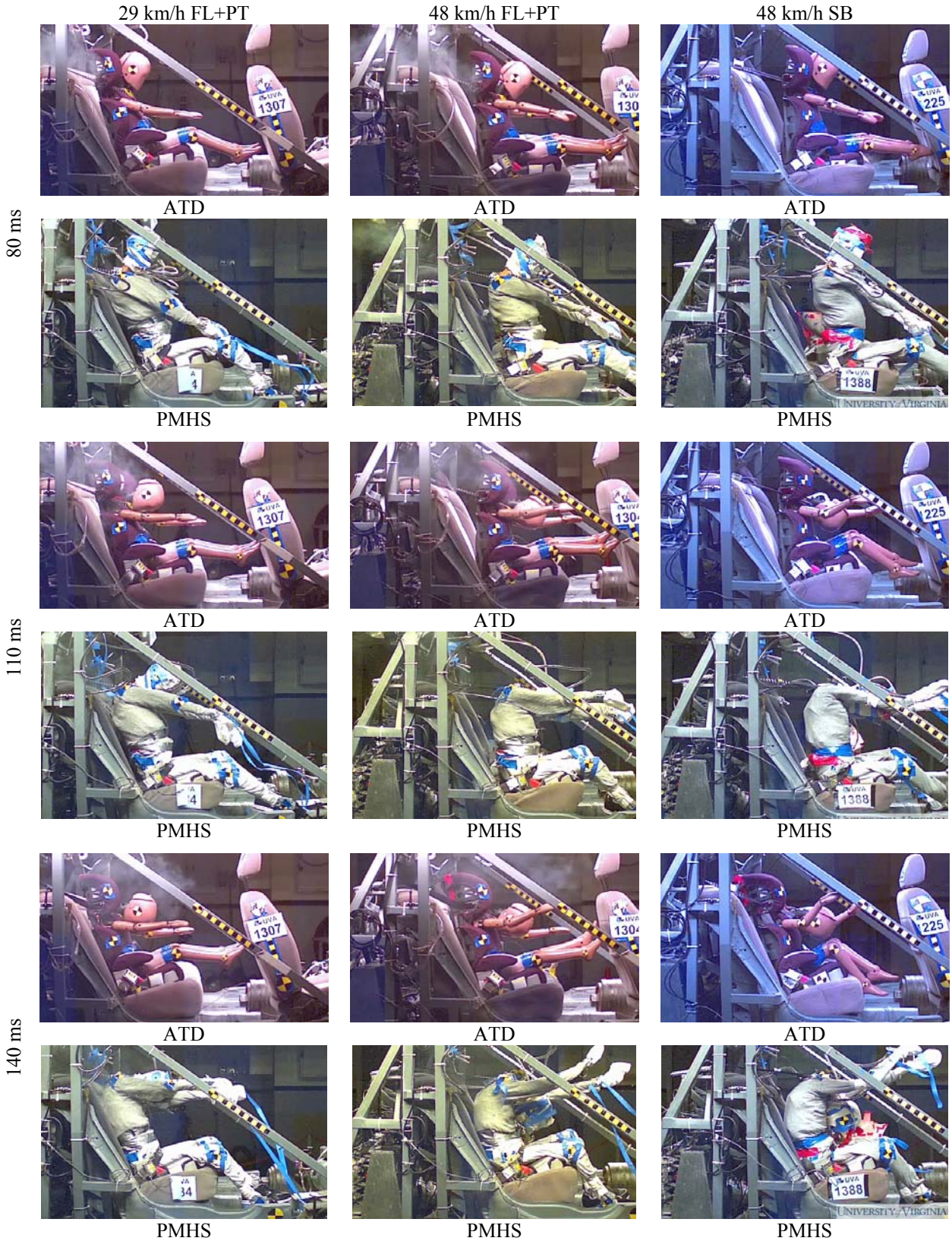

Figure 4 – Comparison between the PMHS and the ATD at different times during the impact.

The line drawing illustrating the occupant contour was scaled with the data to facilitate comparison among the trajectories. In general, the ATD underestimated the maximum displacement of the photo targets of the un-scaled PMHS, which was expectable due to the bigger size of the PMHS. After scaling the PMHS data, the forward excursion of the ATD was actually greater than that of the PMHS in all test conditions. Apart from the magnitude comparison, it was also found that those PMHS body regions that underwent mostly a linear translation were better represented by the ATD (i.e., H point, knee, shoulder at 48 km/h). However, when there was a substantial arc in the motion, the ATD followed a straighter trajectory than the PMHS. This is reflected in the PMHS's generally greater displacements in the Z direction. This trend was observed regardless of scaling the data.

Torso angle (defined as the angle between the chord connecting the shoulder and pelvis markers and the X axis of the buck, see Figure 2) for each condition is plotted as a function of time in Figure 5. The photo target for the H-point in the dummy was sometimes covered by the booster seat armrest, especially during the earlier phases of the impact. This explains the occasional high values of the standard deviation obtained in some of the tests. The plots show that torso angle was not completely correctly predicted by the ATD especially for the high speed cases, where there was a substantial amount of PMHS torso rotation (at 48 km/h with the SB belt, dummy torso angle value corresponding to maximum forward pitch was 110.6 degrees and PMHS angle was 90.4 degrees). Regardless of the restraint used and the speed of the impact, the ATD torso forward pitch was always less than the PMHS pitch. At 48 km/h, the ATD torso angle with the SB belt varied between 126 degrees and 110.6 degrees, while this interval for the PMHS ranged from 110 degrees to 90.4 degrees. Furthermore, the FL+PT belt induced early rearward pitch in the PMHS due to the pretensioner stroke. This effect was hardly captured by the ATD, showing an almost monotonically decreasing trend till the rebound phase started. The image captures in Figure 4 illustrate this difference (see the 80 ms frame, especially for the 29 km/h speed).

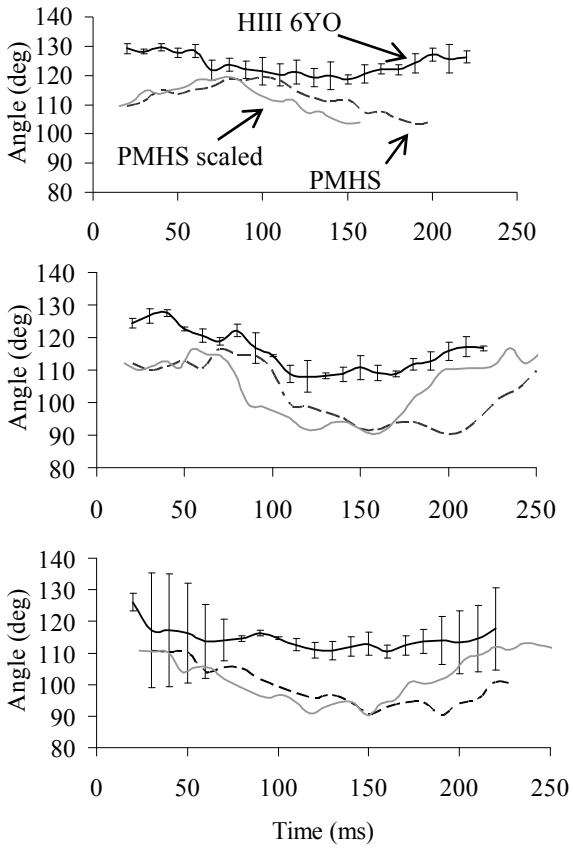

Figure 5 – Torso angle: a) 29 km/h, FL+PT belt, b) 48 km/h, FL+PT belt, c) 48 km/h, SB belt.

The time histories for the upper shoulder seatbelt tension are presented in Figure 6 to Figure 8. The force limiter of the FL+PT belt yielded at both impact speeds (Figure 6 and Figure 7). The pretensioning stroke can be also seen in these plots at t=15 ms. At 29 km/h and with the FL+PT system, the ATD's maximum belt tension was 2428 N at 86 ms. The unscaled PMHS maximum was 2200 N at 88 ms and scaled PMHS was 1351 at 70 ms. Maximum values for the FL+PT tests at 48 km/h were 3072 N at 86 ms for the ATD, 3035 N at 91 ms for the unscaled PMHS and 1870 N at 71 ms for the scaled PMHS. For the SB belt at 48 km/h, seatbelt tension maximum values were 5169 at 76 ms for the ATD, 4528 N at 78 ms and 2790 N at 61 ms. Scaling the forces and time made the force-time history to shrink in time and to diminish in force magnitude. In fact, dummy values were closer to non-scaled PMHS data, despite of the differences in size and weight.

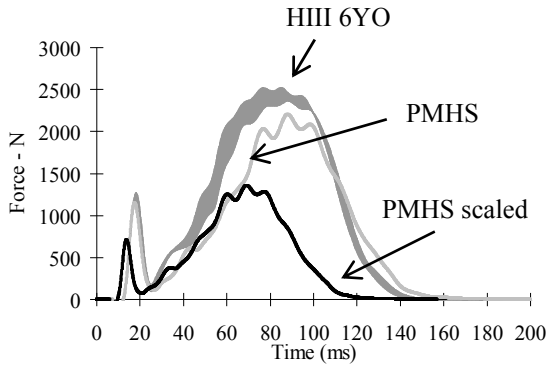

Figure 6 - Upper shoulder belt forces: PT+FL, 29 km/h. (Note: ATD curve corresponds to mean value ± standard deviation)

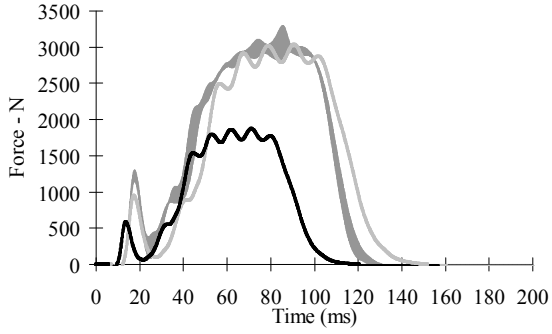

Figure 7 – Upper shoulder belt forces: PT+FL, 48 km/h. (Note: ATD curve corresponds to mean value ± standard deviation)

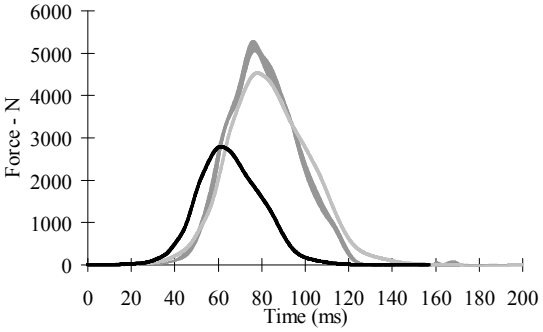

Figure 8 - Upper shoulder belt forces: SB, 48 km/h. (Note: ATD curve corresponds to mean value ± standard deviation)

Peak values of selected data channels for the ATD tests (mean ± standard deviation) and the PMHS test are presented in Table 4. At 29 km/h with the FL+PT belt, the Head Injury Criterion (HIC_{15}) was 46±5 for the ATD and 41 for the PMHS. Maximum peak resultant acceleration at the head cg was, however, greater for the PMHS. In the higher speed tests the ATD underestimated both the HIC and the head cg acceleration of the PMHS regardless of the restraint used. At 48 km/h and with the FL+PT belt, HIC_{15}=368.1 for the PMHS and HIC_{15}=203±22 in the ATD tests. When the SB belt was used, PMHS exhibited a HIC_{15}=481.4 and dummy tests produced a HIC_{15}=457±19. Consistently, maximum peak values of the resultant acceleration at the head CG of the PMHS were higher than the correspondent ATD ones. Both mid-spine (T9 location for the PMHS) and pelvis maximum resultant acceleration values were higher in the PMHS than in the dummies, though the differences between PMHS and dummy were more significant at the mid-spine level.

DISCUSSION

In this study, three frontal sled tests were conducted on a child-size PMHS adult subject. The result of these test have been compared to the outcome of nine tests performed with the Hybrid III 6YO. The objective of this comparison was to assess how the Hybrid III 6YO represented the kinematics of the small PMHS. Since the size of the PMHS was slightly bigger than the 50% percentile 6YO, the comparison between the ATD and the PMHS was done using both unscaled PMHS data and scaled PMHS data. Scaling was based on erect sitting height. Other scaling relationships could have been used, but since the goal of the paper was mainly to compare the kinematics, a length-based scale factor seemed to be more appropriate [Kerrigan et al. 2005]. Both scaled and unscaled belt force data were also presented. For the purposes of comparing the PMHS to the ATD, it is important to note that the overall body mass of the PMHS is closer to the ATD than its overall torso height. Thus, the unscaled force data may be a more valid comparison than the scaled data, especially since these tests were performed without a D-ring and thus minimized the geometrical dependence of the belt force.

In the comparison between the ATD trajectories and the scaled PMHS data, as shown in Figure 3, the ATD slightly overestimated the forward excursion of the PMHS. The seatbelt forces generated by the ATD were also reasonably representative of those generated by the PMHS (unscaled). These results suggest that the Hybrid III 6YO is a useful tool for many applications. However, differences between the ATD and the PMHS were found for other important parameters in the study of the kinematics of the occupant such as peak accelerations or torso angle. Acceleration values for the head CG and mid-

spine were higher for the PMHS in the high speed tests (48 km/h) regardless of the restraint system used, which resulted in a higher HIC_{15} as well. Scaling of these values gave even greater differences between the ATD and the PMHS.

The process of transforming head acceleration from the cube mounted at an arbitrary location and orientation on the head to the head cg presented some challenges. With the instrumentation package used, this transformation requires integration of the rotational velocity. Errors from integration of digital signal are inherently cumulative, so the influence of factors such as signal filtering and skull deformation is important in tests with significant rotational velocity. This influences the estimation of the HIC and of the head cg acceleration in ways that cannot be quantified with the instrumentation used here.

Previous research has highlighted the differences between pediatric PMHS and ATD, especially concerning the influence of the spine on the whole-body kinematics. Kallieris et al. (1976) conducted sled testing on four pediatric PMHS and two child dummies restrained in the same manner (a deformable table and a lap belt). In these tests, seatbelt loads were higher for the ATDs. Also, the head of the ATD moved forward and up farther than the PMHS. This study reported that the main difference in the kinematics between subjects was the flexion of the spine, especially at the level of the thoracic and lumbar spine. Backaitis et al. (1975) compared the response of juvenile baboons (as surrogates of pediatric occupants) and an ATD, using a matched-pair comparison. In these tests, seatbelt forces were found to be higher in the ATDs (though the baboons in this case were lighter than the dummies). Head forward excursion exhibited reasonably similar behavior between the baboons and the ATDs (ATDs sustained a slightly higher excursion).

A later study of Kallieris et al. (1976) tests attributed the differences between PMHSs and ATDs to the rigid spine of the dummies [Sherwood et al., 2003]. The human spine is a relatively mobile, multi-segmented system, while the Hybrid III dummy's thoracic spine is essentially rigid. This is true not only for pediatric ATDs, but also for adult ones [Shaw et al. 2001]. While overall head excursion, for example, may not be sensitive to this factor, difference in spinal compliance can be significant as finer assessment of dynamics, such as torso pitch or neck moment, is made. In this study we have observed similar findings.

Figure 5 shows the evolution of the torso angle in time. The position of the H-point of the occupant during the first instants of the impact was obscured by the armrest of the booster seat, making difficult the assessment of the torso angle in the earliest phases of the crash. In Figure 5a, the pretensioning of the seatbelt made the torso of the PMHS to pitch initially backwards till t=80 ms (scaled), instant in which the torso angle changed from 120º to 103º. In case of the ATD, torso angle ranged between 123º to 119º over the same time interval, showing a stiffer behavior. In case of the higher speed using the FL+PT belt (Figure 5b), at time t=70 ms, the angle values for the PMHS and the ATD were similar (114º and 118º respectively). At that instant, both the PMHS and the ATD started to pitch forward. However while the overall PMHS torso rotation was 24º (minimum torso angle=90º), the ATD torso rotation was only 10º (minimum torso angle=108º). When the SB belt was used, the total amount of torso rotation was lower than with the FL+PT belt (Figure 5c) for both the PMHS and the ATD. In this case, the variability in the estimated ATD torso angle at the beginning of the crash was significant. This variability is reduced around t=80 ms, when the ATD torso angle value was 114º. At this time, the PMHS torso angle was 99º. While the amount of torso rotation for the PMHS was nine degrees, the torso rotation for the ATD was only three degrees. These results show that the ATD presented a more rigid behavior in torso rotation than the PMHS. This is also shown in Figure 4 where images from the high-speed video cameras are compared at different times during the impact. A substantial amount of spine flexion is seen in the PMHS captures. This flexion of the spine could also explain why the resultant acceleration for the head CG (and therefore, HIC_{15} values) as well as at the mid-spine level is underestimated by the ATD. Flexion of the spine would add a rotational component to the acceleration of the body structures that is not present on the dummy.

Ligamentous injuries at the cervical spine can be related to the flexion displacement of the head during the tests (see Figure 4, 48 km/h SB belt, 140 ms). Injuries found include a fracture to the right clavicle and several rib fractures, likely due to the interaction with the restraint system. The discussion on the injuries to the thorax and lower extremities is out of the scope of this paper

Though it was not the focus of the paper, the comparison between different restraint systems to restrain a booster seated small occupant in a rear seat environment is also an interesting finding. There

were no apparent adverse effects of the force-limiting or pretensioning for the conditions tested here. The FL+PT induced less force peak values on the PMHS and did not increase the forward motion of the head or torso. These results are in agreement with those of Forman et al. (2008).

Table 4 – Peak data summary of selected channels (Avg. ± Std. Dev for the ATD's)

	FL+PT						SB		
	29 km/h			48 km/h			48 km/h		
	HIII 6YO	PMHS scaled	PMHS	HIII 6 YO	PMHS scaled	PMHS	HIII 6YO	PMHS scaled	PMHS
Buck acceleration (g)	11.7±0.5	NA	13.8	21.7±.01	NA	22.0	21.±0.13	NA	22.6
Head CG acceleration (g)	32.0±1.4	51.0	40.0	46.0±2.4	104.2	81.8	65.0±0.9	107.5	84.4
HIC 15	46.0±5		41.0	203.0±22.		368.0	457.0±19		481.0
T1 acceleration resultant (g)	NA	69.2	54.3	NA	51.7	40.6	NA	74.9	58.8
Mid-spine acceleration resultant (g)	16.0±1.4	27.8	21.8	29.0±1.7	57.7	45.3	55±1.7	105.5	82.8
Pelvis acceleration resultant (g)	24.0±0.9	27.1	21.3	46.0±4.2	70.5	55.3	53±1.7	87.1	68.4
Upper shoulder belt tension (kN)	2.4±0.1	1.36	2.20	3.1±0.2	1.87	3.04	5.2±0.13	2.79	4.53
Lower shoulder belt tension (kN)	1.5±0.1	0.96	1.56	1.8±0.1	1.21	1.97	3.9±0.11	1.68	2.73
Lap belt tension (kN)	1.4±0.02	0.61	1.00	3.1±0.3	1.65	2.67	3.5±0.3	2.14	3.47

The development of child ATDs has remained a challenge over the last years due to the lack of biomechanical pediatric data. This lack of data has been partially overcome using scaling methods. This study shows that scaling can be used to describe certain aspects of the interaction between a pediatric occupant and the interior of the car during an impact. However, there are still many unknowns to completely describe how a child will behave in real crashes. The development of the spine is a continuous process that is not fully completed until approximately 30 years of age, when the ossification of the vertebrae finishes. The intervertebral disks grow at different rates in different parts of the column [Franklyn et al., 2007]. There are insufficient published data to fully understand the consequences of pediatric spinal development on the flexion-extension of the spine during a frontal impact. Also, the differences in the material properties of the pediatric and adult tissue have not been examined here though they are essential to understand injury causation in children. This may be a significant limitation of our study since the child-size PMHS comprised adult tissue.

A shortcoming of this study was the use of only one PMHS to compare with the ATD tests. PMHS availability is always a critical issue, especially in this anthropometric range. The specific anthropometric characteristics of this subject made it a desirable subject for comparison with pediatric ATDs. The test matrix was designed to allow repeated impacts on the PMHS in order to minimize tissue changes while maximizing the information gleaned from this rare test subject.

CONCLUSION

A comparison between nine frontal sled tests using a Hybrid III 6YO and three tests performed on a small child-size adult PMHS has been performed in this paper. Two different restraint systems (FL+PT and SB) and two different impact speeds (29 km/h and 48 km/h) were evaluated. Data from the PMHS was scaled using the characteristic length of a 50th percentile 6YO. ATD predicted correctly the peak values of the scaled displacements of the PMHS. However, the ATD predictions for other kinematic parameters such as torso angle and resultant accelerations at different locations were found to be different from the PMHS values. The higher stiffness of the ATD spine was proposed as a major cause for these discrepancies.

ACKNOWLEDGMENTS

The authors would like to thank the Association for the Advancement of the Medicine and Biodynamic Research Corp. for their support in the form of the AAAM Student Dissertation Grant. The tests reported here were sponsored by Autoliv Research. The authors also gratefully acknowledge the National Highway Traffic Safety Administration for its support of UVA's broader rear-seat research program and, in particular, Steve Ridella and Shashi Kuppa for their technical insights, guidance, and encouragement. Ford Motor Company supplied

equipment as well as valuable technical input. Specifically, Stephen Rouhana and Priya Prasad deserve our thanks. Finally, Francisco J. Lopez-Valdes acknowledges and thanks Obra Social – Fundación "la Caixa" for their support in the form of an International Graduate Grant.

REFERENCES

Adekoya, N., D. Thurman, D. White and K. Webb (2002). Surveillance for traumatic brain injury deaths--United States, 1989-1998. MMWR Surveill Summ. 51(10): 1-14.

Arbogast, K. B., I. Chen, D. Durbin and F. K. Winston (2004). Injury risks for children in child restraint systems in side impact crashes. IRCOBI Conference, Graz, Austria.

Arbogast, K. B., R. A. Cornejo, M. J. Kallan, F. K. Winston and D. R. Durbin (2002). Injuries to children in forward-facing child restraints. Annu Proc Assoc Adv Automot Med 46: 213-30.

Backaitis SH, Medlin JW, Radovich VG, Stalnaker RL, Shah MP, Shaffer JT, Letscher RM. (1975) Performance evaluation of child dummies and baboons in child restraint systems in a systematized crash environment. Paper No. 751153. Society of Automotive Engineers, 1975.

Brun Cassan, F., Page, M., Pincemaille, Y., Kallieris, D., Tarriere, C. (1993) Comparative study of restrained child dummies and cadavers in experimental crashes. Paper 933105, Society of Automotive Engineers, Warrendale, PA.

Eppinger, R., Marcus, J., Morgan, R. (1984) Development of dummy and injury index NHTSA's thoracic side impact protection research program. Paper No. 840885, 27th Stapp Car Crash Conference.

Forman J, Michaelson J, Kent R, Kuppa S, Bostrom O. Occupant restraint in the rear seat: ATD responses to standard and pre-tensioning, force-limiting belt restraints. Annu. Proc. Assoc. Adv. Automot Med., 2008, 52, 141-154.

Franklyn M, Peiris S, Huber C, Yang KH. Pediatric material properties: a review of human child and animal surrogates. Critical Reviews in Biomedical Engineering, 35(3-4), 1997-342 (2007).

Kallieris D, Barz J, Schmidt G, Heess G, Mattern R. Comparison between child cadavers and child dummy by using child restraint systems in simulated collisions. Paper No. 760815. Society of Automotive Engineers, 1976.

Kallieris, D., Schmidt, G., Barz, J., Mattern, R., Schulz, F. (1978) Response and Vulnerability of the Human Body at Different Impact Velocities in Simulated Three-Point Belted Cadaver Tests. Proc. IRCOBI, pp. 105-209.

Kerrigan, J., Kam, C., Drinkwater, C., Murphy, D.,Bose, D., Ivarsson, J., Crandall, J. (2005) Kinematic comparison of the Polar-II and PMHS in pedestrian impact tests with a sport-utility vehicle. Proc. International Research Council on the Biomechanics of Impact (IRCOBI). Prague,Czech Republic. pp. 159-174.

Malina RM, Hamill PW, Lemeshow S. National Health Examination Survey: Selected Body Measurements of Children 6-11 years. 1963-1965. Washington DC. US Government Printing Office. Vital and Health Statistics Series II, no. 123. DHEW publ. no. (HSM) 73-1605.

Martin, P., Hall, G., Crandall, J., Pilkey, W. (1998) Measuring the acceleration of a rigid body. Shock and Vibration 5:211-224.

Michaelson J, Forman J, Kent R, Kuppa S. Rear seat occupant safety: kinematics and injury of PMHS restrained by a standard 3-point belt in frontal crashes. Stapp Car Crash J., 2008, 52, 295-325.

Robbins DH. (1983) Anthropometric specifications for mid-sized male dummy. Volume 2. University of Michigan Transportation Research Institute (UMTRI) report number UMTRI-83-53-2.

Shaw, C, Kent, R, Sieveka, E, Crandall, J. (2001) Spinal kinematics of restrained occupants in frontal impacts. IRCOBI Conference on the Biomechanics of Impact, Isle of Man.

Sherwood, C., C. Shaw, L. V. Rooij, R. Kent, J. Crandall, K. Orzechowski, M. Eichelberger and D. Kallieris (2003). Prediction of cervical spine injury risk for the 6-year-old child in frontal crashes. Traffic Inj Prev 4(3): 206-213.

Wismans, J., Maltha, J., Melvin, J., Stalnaker, R. (1979) Child restraint evaluation by experimental and mathematical simulation. Paper 791017, Society of Automotive Engineers, Warrendale, PA